Transport barriers in plasmas

2012 J. Phys.: Conf. Ser. 370 012001

(http://iopscience.iop.org/1742-6596/370/1/012001)

Journal of Physics: Conference Series **370** (2012) 012001 doi:10.1088/1742-6596/370/1/012001

Transport barriers in plasmas

I L Caldas[1], J D Szezech Jr[1], T Kroetz[1], F A Marcus[2], M Roberto[3], R L Viana[4] and S R Lopes[4]

1 Institute of Physics, University of São Paulo, São Paulo, Brazil
2 PIIM, Université de Provence, F-13397 Marseille cedex 20, France
3 Aeronautic Institute of Technology, São José dos Campos, Brazil
4 Physics Department, Federal University of Paraná, Curitiba, Brazil

E-mail: ibere@if.usp.br

Abstract. We discuss the creation of transport barriers in magnetically confined plasmas with non monotonic equilibrium radial profiles. These barriers reduce the transport in the shearless region (i.e., where the twist condition does not hold). For the chaotic motion of particles in an equilibrium electric field with a nonmonotonic radial profile, perturbed by electrostatic waves, we show that a nontwist transport barrier can be created in the plasma by modifying the electric field radial profile. We also show non twist barriers in chaotic magnetic field line transport in the plasma near to the tokamak wall with resonant modes due to electric currents in external coils.

1. Introduction

Recently there is a growing interest in non monotonic systems [1, 2, 3], for which the twist condition is not fulfilled for all points in the domain of interest [4]. The non twist condition have been found in many dynamical systems of physical interest, like fluids and plasmas [5, 6, 7, 8, 9, 10].

Nontwist systems present internal transport barriers that play a major role in the study of diffusion in fluids and plasmas [11]. In particular, internal transport barriers are important to separate regions with qualitatively different dynamical behavior. Even after the internal barriers are broken the remaining dimerized islands created by nontwist systems may present high stickness configurations that decreases the transport in the nontwist region [1].

In this work, initially, we introduce the barriers in the standard nontwist map and then we analyze two kinds of problems in plasmas with non-monotonic field profiles: the first is the chaotic particle drift motion caused by electrostatic drift waves; the second problem is the chaotic magnetic field line transport in plasmas with external resonant perturbations.

2. Nontwist standard map

Initially, we present the nontwist transport barrier in the most used symplectic nontwist map, namely, the standard nontwist map (SNTM) introduced in Ref. [6]. The winding number of this map is not monotonic with a twistless surface surrounded by two chain of dimerized islands. This map is given by

$$x_{n+1} = x_n + a(1 - y_{n+1}^2), \quad (1)$$

$$y_{n+1} = y_n + b\sin(2\pi x_n) \pmod 1, \quad (2)$$

where $x \in [-1/2, +1/2)$, $y \in \mathbb{R}$, $a \in (0, 1)$, and $b > 0$.

The function $a(1 - y_{n+1}^2)$ is the winding number of the unperturbed phase-space trajectories lying on nested tori, its derivative being the so-called shear function. If the shear function is monotonically increasing or decreasing for all values of interest, the shear does not change sign and the twist condition is satisfied. The lines where winding number changes sign define the shearless curves in phase space.

Recently there is a growing interest in nontwist maps, some of whose properties are quite different from those known for twist maps, such as the KAM and Aubry-Mather theory [2]. For example, certain periodic islands can interact without overlapping as the perturbation is increased, rather experiencing either a separatrix reconnection process or mutual annihilation after they collide [2,3]. One of the conspicuous features of nontwist maps is the robustness of shearless curves against increasing perturbations, which leads to transport barriers not present in twist maps [1]. In the latter there is a well-known transition from local (separatrix) to global chaos, whereas in nontwist maps separatrix reconnection may or may not lead to global transport depending on the map parameters [1]. The transport barriers of nontwist maps are examples of structures which affect in a global way the transport over a phase space region.

The mathematical properties of SNTM have been extensively investigated over the past two decades [1, 2, 3, 11]. In the following we outline some of these properties, referring to the literature for a more complete coverage of them. In the unperturbed case ($b = 0$) the twist condition is violated at the point $y = 0$, what defines a shearless curve. The quadratic term in (1) leads to two invariant curves with the same winding number at both sides of the shearless curve.

As the perturbation becomes nonzero ($b \neq 0$) two periodic island chains appear at the two invariant curve locations, and the former shearless curve becomes a shearless invariant tori separating these two island chains [1, 2]. There are also chaotic layers attached to both island chains, as expected from the presence of homoclinic crossings therein. These chaotic layers are not connected, though, as far as there are invariant curves near the shearless invariant tori acting as dikes, preventing global transport [1, 2, 11].

In figure 1, where a Poincaré section of the SNTM is depicted for $a = 0.52$ and $b = 0.32$, we observe two island chains with two islands each. The local maxima of the perturbed winding number profile define a shearless invariant curve, whose existence can be inferred between the two island chains. The island chains bordering the shearless invariant curve are transport barriers, since chaotic trajectories above and below do not mix at all [11].

If the parameters are further modified another noteworthy feature of nontwist maps can emerge, depending on the parameter space region. In one scenario (generic reconnection) the island chains with the same winding number approach each other and their unstable and stable invariant manifolds suffer reconnection. In the region between the chains, there appear new invariant tori called meandering curves (which are not KAM tori, though, since the latter must be a graph over x, while meanders are not). The periodic orbits remaining eventually coalesce and disappear, leaving only meanders and the shearless torus.

Further growth of the a-parameter causes the breakup of the transport barrier and the consequent mixing of the chaotic orbits formerly segregated on both sides of the shearless invariant torus.

3. Transport barrier at tokamak plasma edge

In tokamaks the plasma confinement can be improved when the radial electric field profile is modified by a bias electrode [12, 13].

We use a Hamiltonian model to show that the reported transport reduction is caused by displacement of a transport barrier from the scrape-off layer to the plasma edge. For that we consider a large aspect ratio tokamak with $\mathbf{B} = B_0\mathbf{e_z}$, and the particle guiding center drift in

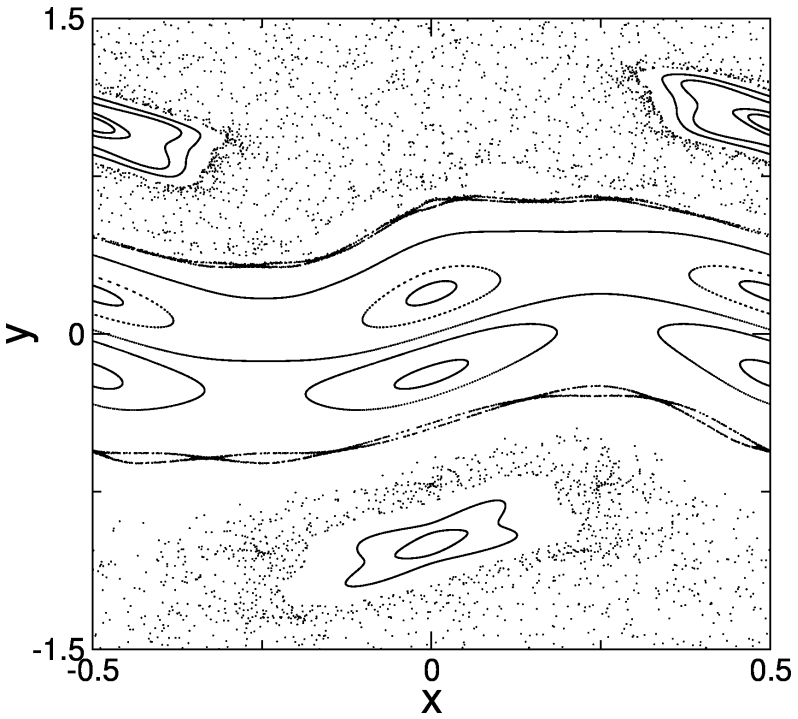

Figure 1. Nontwist map. Phase space with transport barrier for $a = 0.52$ and $b = 0.32$.

poloidal direction given by

$$\mathbf{v}_E = \frac{\mathbf{E} \times \mathbf{B}}{B^2} = \frac{E}{B}\mathbf{e_z}, \tag{3}$$

where x and y stand for the radial and poloidal coordinates respectively. We consider that the observed particle transport at the plasma edge is manly caused by $\mathbf{E} \times \mathbf{B}$ drift [14, 15].

Due to the particle density gradient in the radial direction, a perturbed electric field appears changing the electric field configuration to $\mathbf{E} = E(x)\mathbf{e_x} + \tilde{E}\mathbf{e_y}$, and consequently giving rise to the electrostatic waves, which are responsible to the radial drifts of the particles. We assume an electrostatic potential of the form [16]:

$$\phi(x, y, t) = \phi_0(x) + \sum_i A_i \sin(k_{x_i} x) \cos(k_{y_i} y - \omega t), \tag{4}$$

which is composed of a background equilibrium electrostatic potential, $\phi_0(x)$, with the superposition of a collection of waves propagating in the poloidal direction. By the (3) with $\mathbf{E} = -\nabla\phi(x, y, t)$, we describe the system by the Hamiltonian formalism defining the Hamiltonian by $H(x, y, t) = \frac{\phi}{B_0}$. In this model we use only two waves since this is the minimum to ensure the chaos in the phase space,

$$H(x, y, t) = \phi_0(x) - u_1 x + A_1 \sin(k_{x_1} x) \cos(k_{y_1} y) + A_2 \sin(k_{x_2} x) \cos(k_{y_2}(y - ut)), \tag{5}$$

with $u_1 = \frac{\omega_1}{k_{y_1}}$ being the phase velocity of the first wave and u is the phase velocity difference between the two waves. For equilibrium electric field profiles that are not monotonic, the Hamiltonian system violates the twist condition and it possesses robust invariant tori or barriers that inhibit transport [1]. From the Hamiltonian formalism, we introduce in (6) the trapping

profile U(x) [17]. This function is used to describe the regions with high chaos activity in the phase space where we associate it with high radial particle transport

$$U(x) = \frac{1}{A_1 k_{x1}} \left[\frac{d\phi_0}{dx} - u_1 B_0 \right]. \tag{6}$$

The resonant condition occurs at $U(x) = 0$. Around this value the particle transport is effective, which implies from (6) that the wave phase velocity matches the background drift velocity, $v_E \approx u_1$.

In figure 2 we depict the phase space for a bias discharge. The $U(x) \approx 0$ regions are marked with horizontal sequences of dots, and following those dots to the phase space, we see the chain islands near to the limiter ($x = 1$). Another important issue to notice is the trapping profile maximum point that states the nontwist barrier and it is located inside the plasma ($x = 1$). The dominant wave parameters are the following: $A_1 = 0.084$, $\omega_1 = 7.5$, $k_{y1} = 5.4$, $k_{x1} = 28.3$. The $U(x) = 0$ regions are marked with horizontal sequences of dots, and following those dots to the phase space, we see the chain islands near to the limiter ($x = 1$). Another important issue to notice is the trapping profile maximum point that states the nontwist barrier and it is located inside the plasma ($x = 1$).

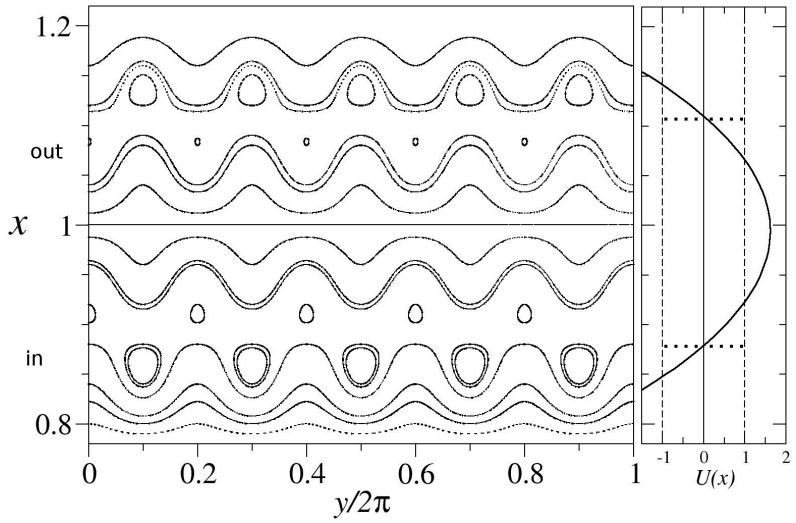

Figure 2. Phase spaces with the trapping profile $U(x)$ aside. The nontwist barrier can be seen where the trapping profile is maximum.

4. Magnetic field line transport

Chaotic field lines at the plasma edge play a key role on plasma-wall interaction in tokamaks [18, 19]. Since charged plasma particles follow magnetic field lines to leading order, one of the undesirable effects of chaotic field lines is the concentration of heat and particle loadings on the tokamak wall that deteriorates the overall plasma confinement quality [20]. Here, we show how the magnetic field line escape to the tokamak wall is affected by the action of a resonant helical perturbation on a tokamak plasma in MHD equilibrium.

In MHD equilibrium the field lines lie on magnetic surfaces, with topology of nested tori. The magnetic surfaces are characterized by a surface quantity which is an approximated analytical solution of the Grad-Shafranov equation in terms of the toroidal non-orthogonal coordinates r_t and θ_t, such that $\Psi \approx \Psi(r_t)$ [21]. The intersections of the flux surfaces $\Psi = constant$ with a toroidal plane are not concentric circles but rather present a Shafranov shift toward the

exterior equatorial region [21]. For the considered coordinate system, $\Psi(r_t)$ is obtained for a monotonical toroidal current density profile, commonly observed in tokamaks discharges, given by $J_\phi(r_t) = \frac{I_p R_0}{\pi a^2} \frac{(\gamma+2)(\gamma+1)}{\beta+\gamma+2} \left(1 + \beta \frac{r_t^2}{a^2}\right) \left(1 - \frac{r_t^2}{a^2}\right)^\gamma$, where I_p and a are the total plasma current and plasma radius, respectively, R_0 is the major tokamak radius, and γ is a positive constant.

We introduce a Hamiltonian formalism, with action and angle variables, to describe the considered integrable equilibrium. However, for a small helical magnetic perturbation the Hamiltonian system becomes almost-integrable [22]. In this work we use an ergodic magnetic limiter (EML) to generate a small localized perturbation, where the explicit dependence on ϕ reflects the break of symmetry [22, 23]. The EML creates resonances in the plasma and it can be designed to excite resonances closer or farther from the tokamak wall, depending on the mode numbers chosen for the limiter winding. To show the perturbed field lines distribution in space, we present a Poincaré map that represents the field line intersections with the toroidal plane $\phi = 0$.

For the present numerical simulations we choose an equilibrium characterized by the following parameters: $a/R_0 = 0.26$ and $b/R_0 = 0.35$, where b is the minor tokamak radius. We also choose $q(a) = 5$ and $q(0) = 1$, corresponding to the safety factors at the plasma edge and magnetic axis, respectively, for which $\gamma = 0.78$ and $\beta = 3.0$. Figure 3 shows the safety factor profile for the considered MHD equilibrium.

Next, we present an example of a transport barrier created by the resonant perturbation considered in this work. We consider that the poloidal and toroidal mode numbers are, respectively, $m_0 = 4$ and $n_0 = 1$. We also normalize lengths to the minor radius ($b = 1$). The results are presented in terms of r and θ variables, more adequate to the comparisons with experimental results. Figure 4 shows a Poincaré map for the limiter currents $I_h/I_p = 2.73$. The island chains due to these resonances although partially destroyed, can be recognized. In the external part of the plasma there are mixed regions with islands and chaotic lines, while more inside the plasma a transport barrier (in red in figure 4) can be identified.

Recent experiments have shown that the radial structure of the electron temperature and density at different times of the discharge reveals a correlation between the field line connection lengths (the number of toroidal turns it takes for a field line to reach the tokamak wall) and the heat flux [20]. There has been observed that most of the heat content is brought from the plasma core wall by the field lines with relatively large connection lengths. The regions with short and long connection lengths are also called laminar and ergodic, respectively [20].

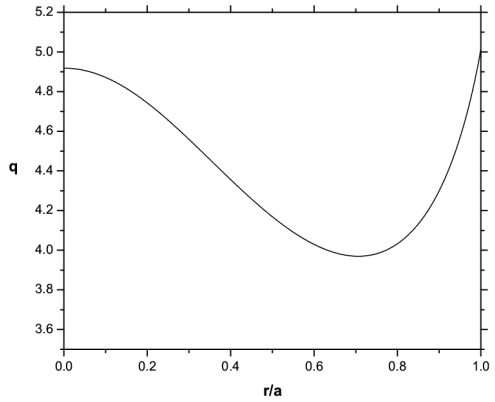

Figure 3. Safety factor profile for the equilibrium considered in this work.

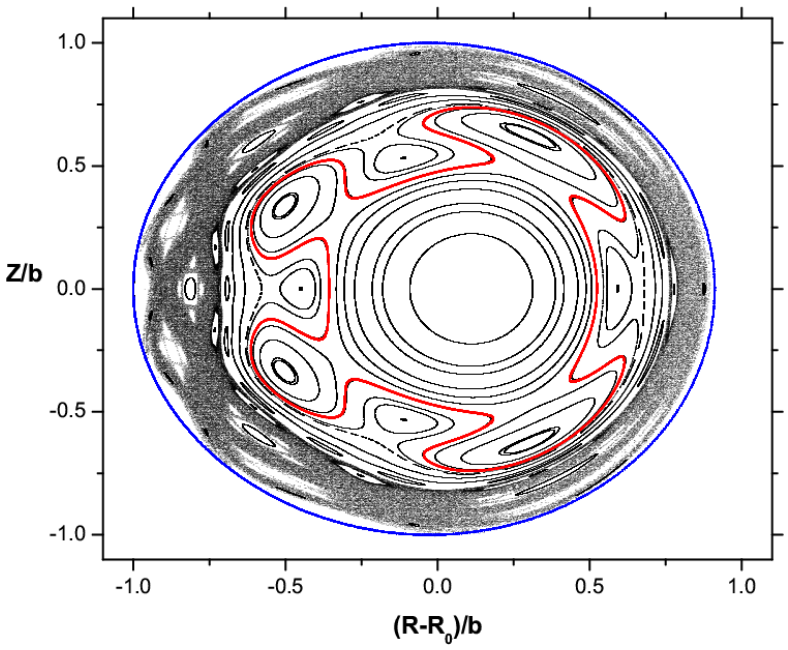

Figure 4. Poincaré section of magnetic field lines inside a tokamak plasma in MHD equilibrium perturbed by an EML.

5. Conclusions

Several applications of the theory of chaos have been reported in the last years to interpret different phenomena observed in tokamak plasmas [24]. Here, we apply the Hamiltonian theory of nontwist dynamical systems to predict the existence of nontwist transport barriers in plasma physics. In [11] we presented examples of such barriers described by plasma models described by symplectic maps. In this article, initially, we give an example of such barriers present in the non Twist Standard Map, a well known paradigm that can be used to investigate qualitatively the onset of transport barriers and their break-up in several systems. Next, we introduce two dynamical systems describing transport in tokamak plasmas with non-monotonic profiles [25]. One system describes the chaotic particle drift motion caused by electrostatic waves; the other system describes the chaotic magnetic field line distribution in plasmas with external resonant perturbations. For these two systems we show how non-monotonic field profiles give rise to transport barriers.

References

[1] Szezech Jr J D, Caldas I L, Lopes S R, Viana R L, and Morrison P J 2009 *Chaos: An Interdisciplinary Journal of Nonlinear Science* **19** 043108
[2] Wurm A, Apte A and Morrison PJ 2004 *Braz. J. Phys.* **34** 1700
[3] Wurm A, Apte A, Fuchss K and Morrison PJ 2005 *Chaos: An Interdisciplinary Journal of Nonlinear Science* **15** 023108
[4] Morrison P J 2000 *Phys. Plasmas* **7** 2279
[5] Kerner W and Tasso H 1982 *Phys. Rev. Lett.* **49** 654
[6] del-Castillo-Negrete D and Morrison P J 1993 *Phys. Fluids* A **5** 948
[7] Horton W, Park H B, Kwon J M, Strozzi D, Morrison P J and Choi D I 1998 *Phys. Plasmas* **5** 39103917
[8] Oda G A and Caldas I L 1995 *Chaos Soliton Fractals* **5** 15
[9] del-Castillo-Negrete D 2000 *Phys. Plasmas* **7** 17021711
[10] Kroetz T, Roberto M, da Silva E C, Caldas I L and Viana R L 2008 *Phys. Plasmas* **15** 092310
[11] Caldas I L, Viana R L, Szezech Jr J D, Portela J S E, Fonseca J, Roberto M, Martins C G L and da Silva E J 2012 *Comm. Non. Science Num. Sim.* **17** 2021

[12] Nascimento IC *et al* 2005 *Nuclear Fusion* **45** 796
[13] Van Oost G et al. 2003 *Plasma Physics Control. Fusion* **45** 621
[14] Ritz C P *et al* 1989 *Physical Review Letters* **62** 1844
[15] Ritz C P, Lin HT, Rhodes L, and Wootton AJ 1990 *Physical Review Letters*, **65** 2543
[16] Horton W 1985 *Plasma Physics and Controlled Fusion* **27** 937
[17] Marcus FA, Caldas I L, Guimaraes-Filho Z O, Morrison P J, Horton W, Kuznetsov Y K and Nascimento I C 2008 *Physics of Plasmas* **15** 112304
[18] Jakubowski M W *et al* 2006 *Phys. Rev. Lett.* **96**, 0350041
[19] Evans T E *et al* 2004 *Phys. Rev. Lett.* **92** 235003
[20] Jakubowski M W, Abdullaev S S, Finken K H, Lehnen M and TEXTOR Team 2005 *J. Nucl. Mat.* **176** 337
[21] Kucinski M Y and Caldas I L 1987 *Z. Naturforsch A: Phys. Sci* **42** 1124
[22] Caldas I L, Viana R L, Araujo M S T, Vannucci A, da Silva E C, Ullmann K and Heller M V A P 2002 *Braz. J. Phys.* **32** 980
[23] Ghendrih Ph *et al* 2002 *Nucl. Fusion* **42**, 1221
[24] Viana R L , da Silva E C, Kroetz T, Caldas I L, Roberto M and Sanjuan M A F *Phil. Trans. Royal Society* (to be published)
[25] Kroetz T, Marcus F A, Roberto M, Caldas I L and Viana R L 2009 *Computer Physics Communications* **180** 642